J. Cell. Mol. Med. Vol 15, No 2, 2011 pp. 209-219

Ferroportin 1 is expressed basolaterally in rat kidney proximal tubule cells and iron excess increases its membrane trafficking

Natascha A. Wolff [a, #], Wei Liu [b, #], Robert A. Fenton [c], Wing-Kee Lee [a], Frank Thévenod [a, *], Craig P. Smith [b, *]

[a] *Department of Physiology & Pathophysiology, University of Witten/Herdecke, Witten, Germany*
[b] *Faculty of Life Sciences, University of Manchester, Manchester, UK*
[c] *The Water and Salt Research Center, Institute of Anatomy, University of Aarhus, Aarhus, Denmark*

Received: June 3, 2009; Accepted: November 18, 2009

Abstract

Ferroportin 1 (FPN1) is an iron export protein expressed in liver and duodenum, as well as in reticuloendothelial macrophages. Previously, we have shown that divalent metal transporter 1 (DMT1) is expressed in late endosomes and lysosomes of the kidney proximal tubule (PT), the nephron segment responsible for the majority of solute reabsorption. We suggested that following receptor mediated endocytosis of transferrin filtered by the glomerulus, DMT1 exports iron liberated from transferrin into the cytosol. FPN1 is also expressed in the kidney yet its role remains obscure. As a first step towards determining the role of renal FPN1, we localized FPN1 in the PT. FPN1 was found to be located in association with the basolateral PT membrane and within the cytosolic compartment. FPN1 was not expressed on the apical brush-border membrane of PT cells. These data support a role for FPN1 in vectorial export of iron out of PT cells. Furthermore, under conditions of iron loading of cultured PT cells, FPN1 was trafficked to the plasma membrane suggesting a coordinated cellular response to export excess iron and limit cellular iron concentrations.

Keywords: iron homeostasis • kidney • ferroportin 1 • proximal tubule • epithelial transport

Introduction

Ferroportin 1 (FPN1) is an iron exporter expressed in a spectrum of tissues including liver, duodenum and in reticuloendothelial macrophages [1–4]. It has been identified as a major modulator of mammalian iron balance [5, 6] since mutations in FPN1 cause haemochromatosis [6]. In addition, hepcidin has been proposed to bind to FPN1, causing internalization and degradation of FPN1, and consequently bringing about a decrease in enteric absorption of inorganic iron [7]. FPN1 is expressed on the basolateral plasma membrane of enterocytes [2, 8] and has been suggested to mediate export of iron out of intestinal epithelial cells [9]. Hephaestin is required for this action [10]. FPN1 mRNA and protein have been detected in kidney [1, 3], yet the renal function of FPN1 is currently obscure.

Previously, we have shown that divalent metal transporter 1 (DMT1) is expressed in proximal tubule (PT) late endosomes and lysosomes and that *in vivo* DMT1 expressed in the PT is strongly modulated in response to changes in dietary iron. We have suggested that following receptor mediated endocytosis of transferrin filtered by the glomerulus, PT DMT1 contributes to the transit of iron across the PT epithelium by exporting iron, liberated from transferrin, across the late endosomal/lysosomal membranes into the cytoplasm [11–13].

The possibility that in the healthy organism iron is filtered by the glomerulus has for many years been disregarded due to the fact that transferrin has an exceptionally high binding affinity for iron and iron bound to transferrin is not filtered. This fact is also the seat of considerable dispute over the notion of non-transferrin bound iron. However, in recent years evidence has come to light suggesting that some transferrin and iron actually make it through the glomerular filter [14–18]. Furthermore, cubilin and transferrin receptor 1, both effective in binding and internalizing transferrin, have been shown to be expressed on the apical, post-glomerular urine facing, membrane of PT cells [19, 20]. One interpretation of these findings is that a new as yet undefined system exists in PT cells for reabsorbing protein bound iron filtered by the glomerulus [21]. An essential part of this mechanism is suggested to be a means of translocating iron across the basolateral membrane (BLM) of PT cells [21]. FPN1 located on the BLM of PT cells could potentially fulfil this role.

[#]These authors equally contributed to the study.
*Correspondence to: Dr. Craig P. SMITH,
Faculty of Life Sciences, University of Manchester,
Manchester, M13 9PT, UK.
E-mail: Craig.smith@manchester.sc.uk

doi:10.1111/j.1582-4934.2009.00985.x

Therefore, the first aim of the current study was to definitively determine the cellular distribution of FPN1 in rat kidney PT in order to gain an insight into the possible function of FPN1 in this critical part of the nephron. Moreover, the second aim of the study was to determine the effect of iron excess or deficit on PT FPN1.

Methods

RT-PCR

Total RNA extraction and reverse transcription were as previously described [12]. Following reverse transcription of total RNA isolated from rat duodenum, rat kidney or Wistar-Kyoto Proximal Tubule-0293 Cl.2 cells, PCR was performed with the following FPN1 targeted primer pairs: sense FPN1P1 5′-TGG TCC TGG GAG CCA TCA TTG GTG ACT G-3′ (GenBank accession no., AF231120, nucleotides 488–515) and antisense FPN2P1 5′-ACG CAC ATG GAC ACC AAA TTC CAA CCA G-3′ (nucleotides 896–923, AF231120),; and sense FPN1P2 5′-CTC TGG AAG GTT TAC CAG AAG ACC CCT G-3′ (nucleotides 937–964, AF231120) and antisense FPN2P1 5′-CTG AGG ATG GAA CCA CTC AGT CCC TGA G-3′ (nucleotides 1271–1298, AF231120). The predicted fragment sizes were 436 bp and 362 bp, respectively. The resultant products were separated on 2% agarose gels containing 0.01% GelRed (Biotium, Hayward, CA, USA), loading 10 μl PCR reactions per lane and viewed under UV light.

Antibodies

Polyclonal FPN1 antiserum targeting peptide sequence NH_2-CAPDEKEV-IDESQPNTSVV-COOH corresponding to amino acids 552–570 of rat FPN1 (GenBank accession no. AAK77858), termed Liu-FPN1, was raised in rabbits. The anti-NBCe1-A antibody (termed 'α-333') has been previously characterized [22].

Xenopus oocytes expression

Mouse FPN1 plasmid was a kind gift from Dr. D.J. Haile Department of Medicine, University of Texas, San Antonio, TX, USA. Xenopus oocytes were prepared and injected as previously described [23] with mouse FPN1 cRNA. Oocytes were then fixed 2–3 hrs in Bouin's solution, cryoprotected in 30% sucrose (3 × 30 min. washes at room temp, then left at 4°C overnight) and 10 μm cryosections where then cut. Oocytes were stained using the previously described protocol [11].

Preparation of membrane fractions and immunoblotting

Crude membrane samples were prepared from male Sprague-Dawley rat kidney or duodenum as previously described [11]. For isolation of BLMs from rat renal cortex two protocols were combined [24, 25]. Cortices from five rats were homogenized and the microsomal fraction was mixed with Percoll (15% w/v), and centrifuged at 48,500 × *g* for 30 min. Fractions 13–17 from the top ('bottom fraction') were enriched in BLM and pooled. The protein concentration was determined by the Bradford method [26]. Samples were incubated with three times loading buffer for 10 min. at 65°C prior to SDS-PAGE. Immunoblotting was performed as described previously [12] using Liu-FPN1 (1:100–1:1000), and α-333 (1:500). Goat anti-rabbit horseradish peroxidase-conjugated secondary antibody (Dako, Glostrup, Denmark) was used at 1:5000 for western analysis and 1:200 for immunostaining.

Immunostaining

Immunohistochemistry: The process for rodent tissue fixation and staining techniques has been described in detail earlier [27]. Light microscopy was carried out with a Leica DMRE microscope (Leica Microsystems, Herlev, Denmark).

Preparation of tissue for immunogold electron microscopy: Fixed tissue blocks from rat kidney cortex were infiltrated with 2.3 M sucrose for 30 min. and frozen in liquid nitrogen. Frozen tissue blocks were subjected to cryosubstitution and Lowicryl HM20 embedding. Staining was performed as previously described [28].

Immunofluorescence labelling of FPN1 of cultured cells

For immunofluorescence labelling of FPN1 in fixed and permeabilized cells the method was as described previously [12] except a 1:500 dilution of secondary antibody was used and H-33342 was used at 0.8 μg/ml. Experiments with non-permeabilized cells were performed according to Wolff *et al.* [29] with the following modifications: Cells grown on cover slips were incubated at 4°C with primary antibody (dilution of Liu-FPN1 1:100 in Ca^{2+}/Mg^{2+}-containing PBS and 0.1% bovine serum albumin), fixed and incubated with secondary Alexa Fluor® 488-conjugated secondary antibody diluted in blocking buffer (1:500) for 90 min. (22°C). Quantitative determination of FPN1 surface fluorescence in WKPT-0293 Cl.2 cells followed a protocol described elsewhere [29].

Cell culture

An immortalized cell line from the S1-segment of rat PT (WKPT-0293 Cl.2) [30] was cultured as previously described [13]. Cells were passaged (passage number <41) twice a week upon reaching confluence.

Iron-loading and -depletion protocols

One day after cell plating (24 hrs), medium was exchanged for complete culture medium containing either 100 μM of ferric ammonium citrate (FAC) or desferrioxamine (DF) and incubated for 36 hrs [31, 32].

Cellular iron content

Iron content of control, FAC- and DF-treated WKPT-0293 Cl.2 cells was essentially performed as described elsewhere [33, 34]. For measurements of iron content 3×10^4 cells/cm^2 were seeded in 25 cm^2 flasks for FAC or 4×10^4 cells/cm^2 in 75 cm^2 flasks for DF treatment. Total cellular iron in

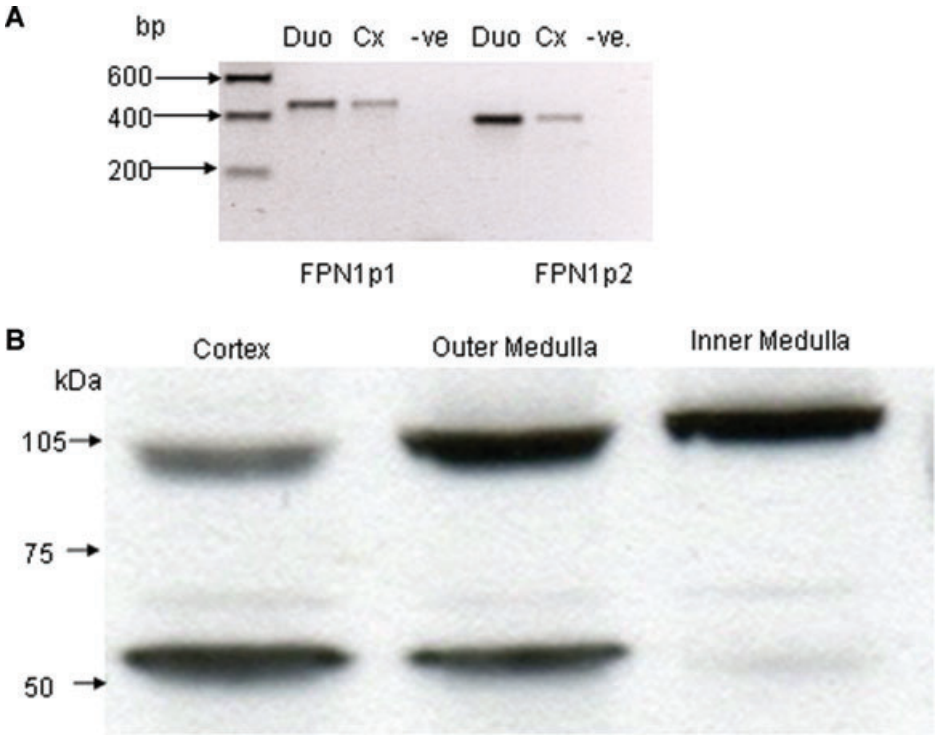

Fig. 1 (**A**) RT-PCR analysis of rat duodenum or kidney cortex total RNA. Duodenum (Duo) yielded products of 436 bp and 362 bp in size using primer sets FPN1p1 and FPN1p2, respectively. Products of the same size were also generated in the kidney cortex (Cx). No products were detected in negative controls (−ve.) which were performed without reverse transcriptase in RT reaction. The positions of size markers are shown on the left in base pairs. (**B**) Immunoblotting of rat kidney membrane fractions using Liu-FPN1 antiserum. Crude membranes isolated from kidney cortex, outer medulla, or inner medulla, were separated by SDS-PAGE on a 12% gelE. An immunoreactive signal was detected at 60 kD in cortex, outer medulla and to a lesser extent in inner medulla. An 110 kD immunoreactive band was also observed in protein from all three regions. Exposure time was 5 min.

FAC-treated cells was 6.53 ± 1.25 nmol/10^6 cells compared to 1.05 ± 0.04 nmol/10^6 cells in the respective controls ($n = 3$; means ± S.E.M.; $P = 0.006$ using unpaired Student's t-test). When cells were treated with DF iron content decreased to 0.88 ± 0.01 nmol/10^6 cells compared to 1.16 ± 0.08 nmol/10^6 cells ($n = 3$; means ± S.E.M.; $P = 0.012$ using unpaired Student's t-test).

Surface biotinylation

Biotinylation of cell surface proteins was conducted using the Pierce® Cell Surface Protein Isolation Kit (Thermo Scientific, Rockford, IL, USA) following manufacturer's instructions with the following modification: At the end of treatment, WKPT-0293 Cl.2 cells were harvested by trypsinization and incubated with freshly dissolved biotin/PBS for 1 hr at 4°C. Protein concentration was determined using the method of Lowry [35] and proteins were detected by immunoblotting. Densitometry analysis was performed with TINA version 2.09 software environment for image analysis research (http://www.tina-vision.net).

Results

Using RT-PCR we confirmed the presence of FPN1 mRNA in rat duodenum and rat kidney cortex. Figure 1(A) shows the single bands of 436 bp and 362 bp generated by amplification using the FPN1P1 and FPN1P2 primer sets, respectively. Sequencing of the PCR products confirmed their identity as rat FPN1 cDNA fragments. Rat duodenum total RNA served as a positive control, while the negative control reactions performed without reverse transcriptase did not give rise to PCR products. The result indicated that FPN1 mRNA is present in rat kidney cortex and that the FPN1 cDNAs generated did not differ from those amplified from duodenum.

To enable the study of FPN1 expression and location, we generated a rabbit polyclonal antibody to the C-terminus of rat FPN1 and affinity purified the antiserum using the immunizing peptide. The resulting antiserum, termed Liu-FPN1, when used for immunoblotting of rat duodenum detected a single strong band of ~60 kD. Incubation of the Liu-FPN1 with immunizing peptide was found to ablate the ~60 kD signal (Fig. S1A). This indicated that Liu-FPN1 antiserum bound to the epitope to which it was raised. To confirm the specificity of Liu-FPN1 we heterologously expressed mouse FPN1 in Xenopus oocytes. Oocytes were then cryosectioned and immunostained with Liu-FPN1. FPN1 expressing oocytes showed strong membrane staining when incubated with Liu-FPN1, whereas membranes of water injected control oocytes treated in the same way were devoid of signal (Fig. S1B and C). These data demonstrate that Liu-FPN1 detects FPN1 protein. To further confirm the capacity of Liu-FPN1 to detect FPN1, we performed immunoperoxidase staining of rat duodenum sections because FPN1 is expressed in BLMs of duodenal enterocytes [2, 4, 8]. Liu-FPN1 strongly stained duodenal villi and staining was not observed following pre-incubation with the immunizing peptide (Fig. S1D). At higher magnification, Liu-FPN1 was observed to strongly stain basal and lateral membranes of duodenal enterocytes

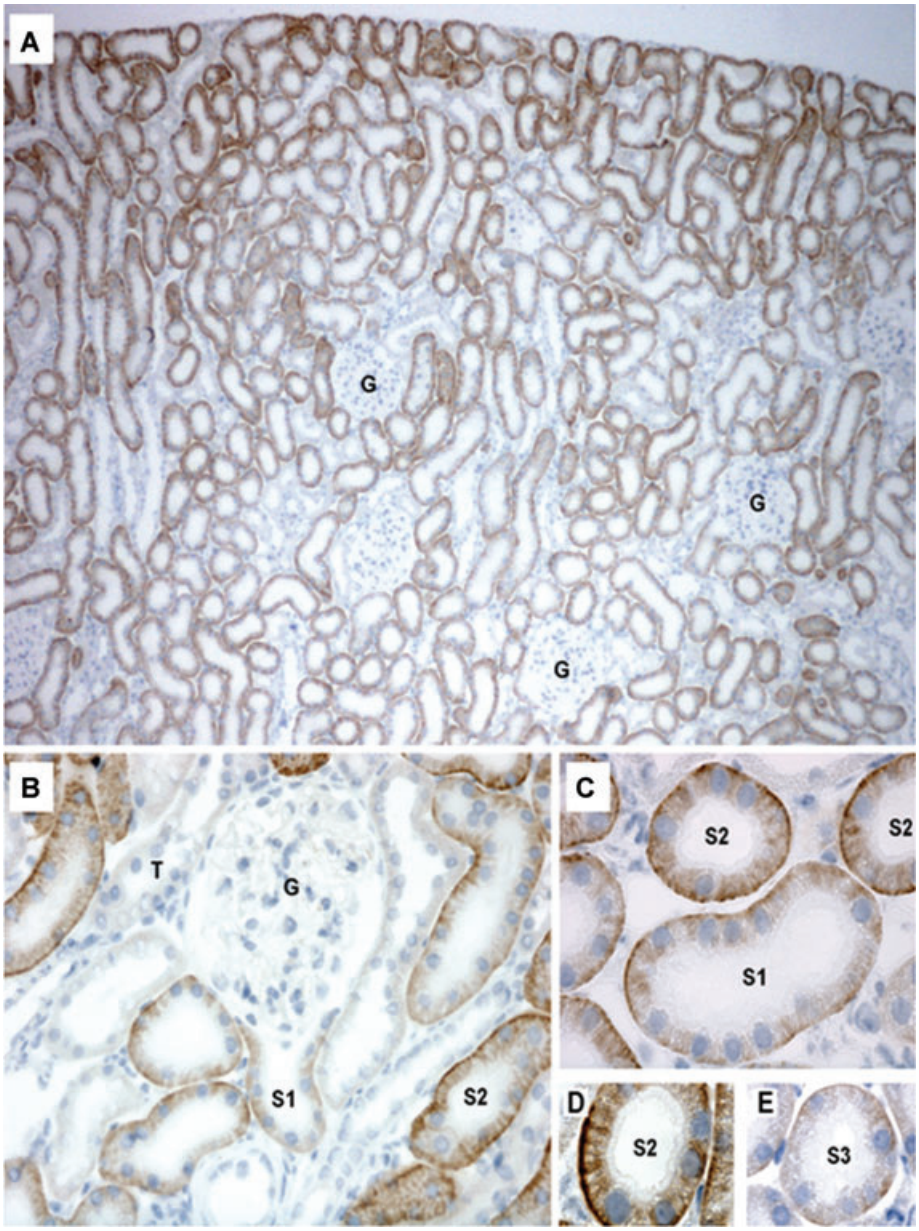

Fig. 2 Immunoperoxidase labelling of Liu-FPN1 in rat kidney. (**A**) Strong labelling is evident throughout the cortex and outer stripe of the outer medulla. Labelling is associated with tubule segments morphologically resembling PTs. No staining is observed in glomeruli or vasculature. (**B**) At high magnification, labelling is predominantly BLM associated, with some intracellular staining. (**C**) and (**D**) Labelling is strongest in the S1 and S2 segments, whilst weaker labelling is observed in the S3 segment (**E**). T, thick ascending limb; G, glomerulus. Immunogold electron microscopy of Liu-FPN1 in rat kidney. (**F**) In PT S1 segments (note the long, extensive invaginations of the basolateral plasma membrane), immunogold labelling of FPN1 is observed throughout the cells basolateral plasma membrane domains (arrows). (**G**) At high magnification FPN1 can be observed in direct association with the plasma membrane. (**H**) In PT S2 segments (note the numerous small lateral processes at the base of the cell), labelling is again observed in direct association with the basolateral plasma membrane. Gold particles are 10 nm. (**I**) FPN1 and kidney electrogenic Na-bicarbonate cotransporter-1 (NBCe1-A) immunoreactivity in rat kidney cortex. Homogenate, microsomal membranes and BLM from rat kidney cortex were separated under reducing conditions by SDS-PAGE on an 8% acrylamide gel. The blot was incubated with anti-rat FPN1 or anti-rat NBCe1-A (1:500). Characteristic bands at ~60 and ~130 kD for FPN1 and NBCe1-A were detected. Sizes (in kilodaltons) of molecular mass markers are indicated on the left.

[2, 8] (Fig. S1E). No staining was present on the apical membrane of duodenal cells. These data clearly define that Liu-FPN1 is selective for FPN1 and is suitable for immunoblotting and immunostaining aimed at detecting FPN1.

To determine the general expression pattern of FPN1 in the kidney, we employed immunoblotting and analysed crude membrane homogenates from the three principal regions of the kidney, namely the cortex, outer medulla and inner medulla of the kidney. The antibody detected a strong ~60 kD protein species in cortex and outer medulla, and a weaker ~60 kD signal in inner medulla (Fig. 1B). A faint protein signal at ~65 kD was also evident in all three kidney regions. An additional strong protein band was also observed in all three regions at ~110 kD.

To visualize the exact cellular location of FPN1 in kidney PT, we immunostained kidneys using Liu-FPN1. Immunoperoxidase staining showed that Liu-FPN1 strongly stained PTs in the kidney cortex. Staining was absent from glomeruli and distal tubules (Fig. 2A). At higher magnification, FPN1 immunoreactivity was observed on the basal membrane and what appeared to be the inside of PT cells (Fig. 2B and C). This pattern of staining was evident in the S1, S2 and S3 segments of the PT (Fig. 2D and E). Staining appeared to be most prominent

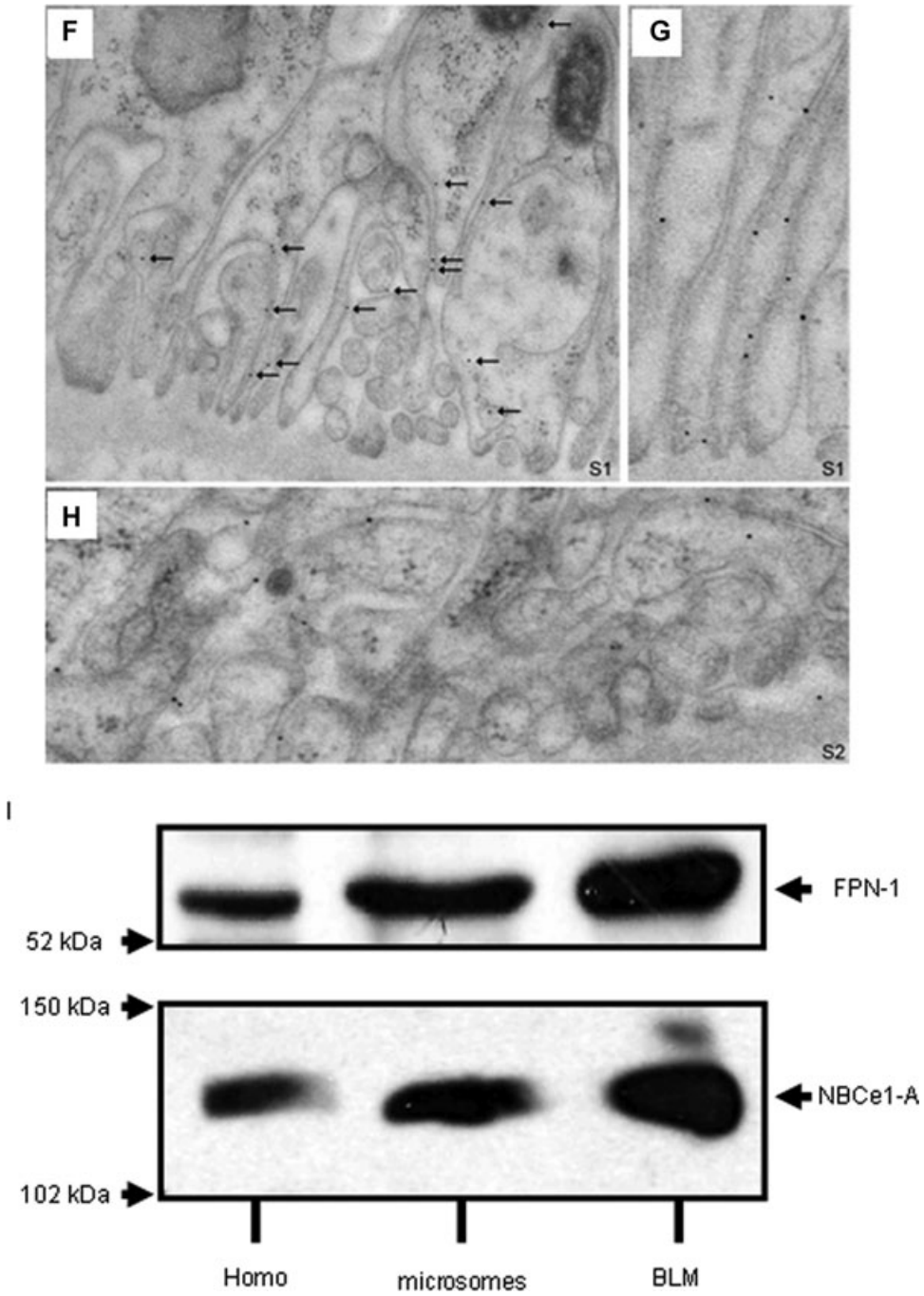

Fig. 2 Continued.

in the S2 segments, weaker in S1 segments and weakest in S3 segments.

Using immunogold electron microscopy enabled us to pinpoint the location of FPN1 immunoreactivity in PT cells. Immunogold particles corresponding to FPN1 protein were observed at the basal and lateral membranes of PT cells, and in addition in the intracellular compartment (Fig. 2F–H and S2). There was no staining of the apical brush-border membrane indicating that FPN1 is unlikely to mediate transport across this membrane. To further confirm the basolateral location of FPN1 we prepared BLM enriched fractions using Percoll gradient preparative centrifugation and compared FPN1 expression levels with cell homogenates. As shown in Fig. 2I, BLM of rat kidney cortex were enriched for FPN1 and co-purified with NBCe1-A, which is highly expressed in

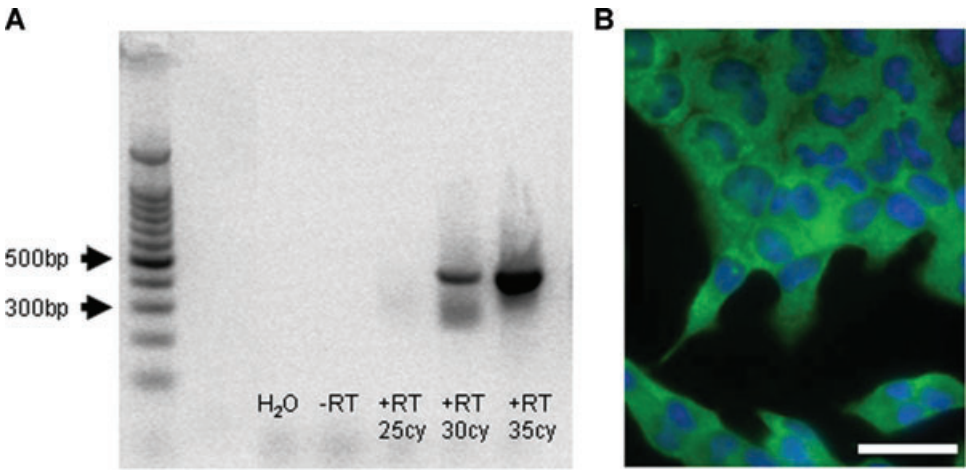

Fig. 3 RT-PCR analysis of total RNA from rat WKPT-0293 Cl.2 PT cells. (**A**) A product of 436 base pairs (bp) in size was obtained using primer sets for FPN1. PCR of FPN1 was performed at 25, 30 and 35 cycles (cy). No products were detected in negative controls which were performed without reverse transcriptase in RT reaction (–RT) or with water instead of template (H_2O). The positions of size markers are shown on the left in base pairs. (**B**) Immunofluorescence staining of PT cells for FPN1. Cells were fixed and permeabilized prior to application of primary anti-FPN1 antibody (1:100) and secondary antibody. (**C**) Immunofluorescence labelling of FPN1 in non-permeabilized in WKPT-0293 Cl.2 cells. Cells were left untreated or exposed to 100 μM FAC or 100 μM DF for 36 hrs. Cells were stained with (upper panel) or without (lower panel) primary anti-FPN1 antibody (1:100) prior to paraformaldehyde fixation. Weak surface expression of FPN1 is seen in controls and DF-treated cells, whereas FAC exposure increases surface staining for FPN1. In the absence of primary antibody only weak background fluorescence was detected. Bars, 30 μm. (**D**) Surface expression of FPN1 in PT cells. Surface FPN1 expression was detected using Alexa Fluor® 488-conjugated secondary antibodies by immunofluorescence microscopy, and mean fluorescence intensity per cell was calculated as described under 'Methods'. Means ± S.E.M. of 28–39 microscopic fields from five experiments are shown. Significant differences to controls were calculated using one-way ANOVA.

the BLM of kidney PT [36]. Therefore, taken together our data conclusively show that FPN1 is expressed at the BLM in PT cells with some intracellular expression. FPN1 was not expressed in association with the apical brush-border.

Our second aim was to determine the affect of iron excess or deficit on PT FPN1. For this we used an established cell model of PT the WKPT-0293 Cl.2 cell line [12, 29, 30]. Firstly, we determined by RT-PCR and immunostaining that FPN1 mRNA and FPN1 protein were present in WKPT-0293 Cl.2 cells. FPN1 cDNA was detected in WKPT-0293 Cl.2 cells using the FPN1P1 primer set (Fig. 3A), FPN1 protein by immunoblotting of total cell homogenates (Fig. 4A) and immunofluorescence staining of fixed and permeabilized confluent cells (Fig. 3B). Therefore, FPN1 is also expressed in the WKPT-0293 Cl.2 cells.

We then investigated whether changes in the iron status of the cultured PT cells affected FPN1. WKPT-0293 Cl.2 cells were exposed to 100 μM FAC for 36 hrs to encourage iron-loading or DF for the same period to promote iron-depletion. FAC significantly increased total cellular iron content by about 600% compared to controls. DF treatment significantly reduced total cellular iron content by ~25% (see 'Methods'). Neither FAC nor DF affected FPN1 mRNA expression (data not shown). Similarly total FPN1 protein expression was not affected by any of the treatments (Fig. 4A). This is in contrast to expression of DMT1, where DMT1 protein was found to be reduced by iron loading (data not shown), and as previously demonstrated *in vivo* [11, 37]. However, FAC treatment resulted in a dramatic increase of FPN1 surface localization, as demonstrated by immunofluorescence staining of non-permeabilized WKPT-0293 Cl.2 cells, whereas DF had no effect (Fig. 3C, upper panel, and 3D). Experiments without primary antibody confirmed that staining was specific (Fig. 3C, lower panel). These observations were confirmed by surface biotinylation of kidney cortex membrane proteins followed by immunoblotting to determine FPN1 expression. FAC increased surface expression of FPN1 3.4 ± 0.7-fold ($P = 0.005$; $n = 5$), whereas DF had no significant effect (0.7 ± 0.4-fold; $P = 0.710$; $n = 5$). Total FPN1 expression in respective cell lysates was not significantly affected by FAC (1.3 ± 0.4-fold; $P = 0.410$; $n = 9$) or DF (1.6 ± 0.8-fold; $P = 0.209$; $n = 6$) (Fig. 4A and B). These data indicate that iron-loading increases FPN1 surface membrane expression in WKPT-0293 Cl.2 cells without affecting total FPN1 expression, indicating redistribution of FPN1 transporters from an intracellular location to the plasma membrane.

Discussion

FPN1 is an iron transport protein that is expressed in several tissues including duodenum, liver and macrophages. It functions as an iron exporter and has been suggested to be a major point of control of iron entry into the circulating transferrin bound iron pool [1–4].

FPN1 mRNA or protein has been detected in kidney [1–3], yet the role of this protein in this tissue, an organ not overtly associated with handling inorganic iron, remains unclear. We therefore set out to firstly determine the cellular location of FPN1 in rat kidney PT as a first step to determine its role in this critical renal structure. Secondly, we determined whether renal FPN1 responded

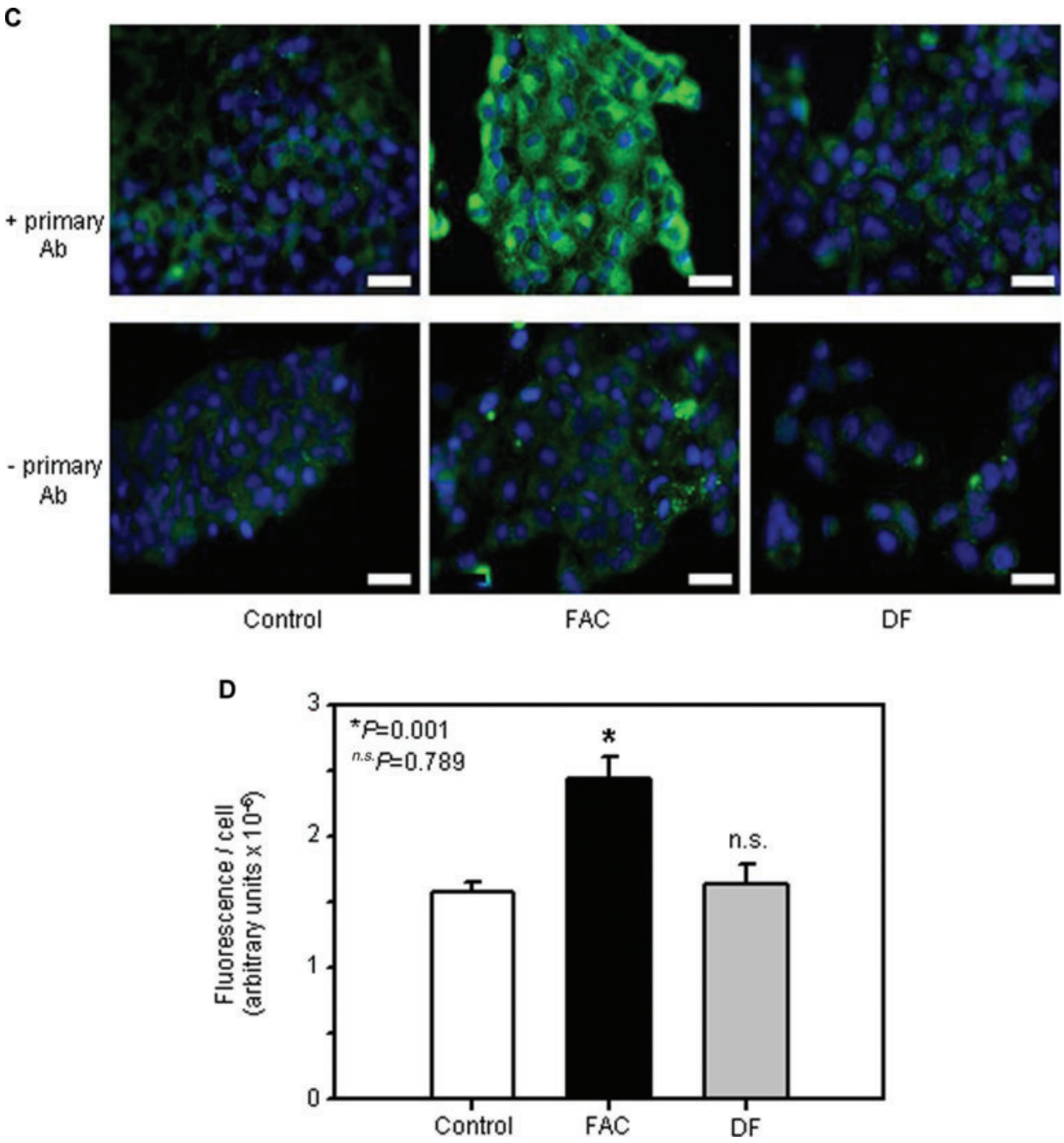

Fig. 3 Continued.

to iron excess or iron deficit, as would be predicted if the protein was in some way involved in iron balance.

RT-PCR analysis of kidney cortex mRNA clearly showed the presence of FPN1 mRNA. PTs account for the majority of tissue in the kidney cortex from which total RNA was extracted. However, glomeruli, distal tubules and connecting tubules, as well as small amounts of endothelial cells, blood cells and smooth muscle cells were also present in the kidney cortex RNA pool we used for our analysis. Therefore, to pinpoint expression of FPN1 in the kidney cortex we raised a peptide targeted antiserum, Liu-FPN1, to the C-terminus of rat FPN1. In crude membrane protein extracts from duodenum, Liu-FPN1 identified a ~60 kD protein. This is in keeping with previously published work that documents FPN1 as a ~60–70 kD protein [4, 38, 39]. In fact, FPN1 cDNA (GenBank

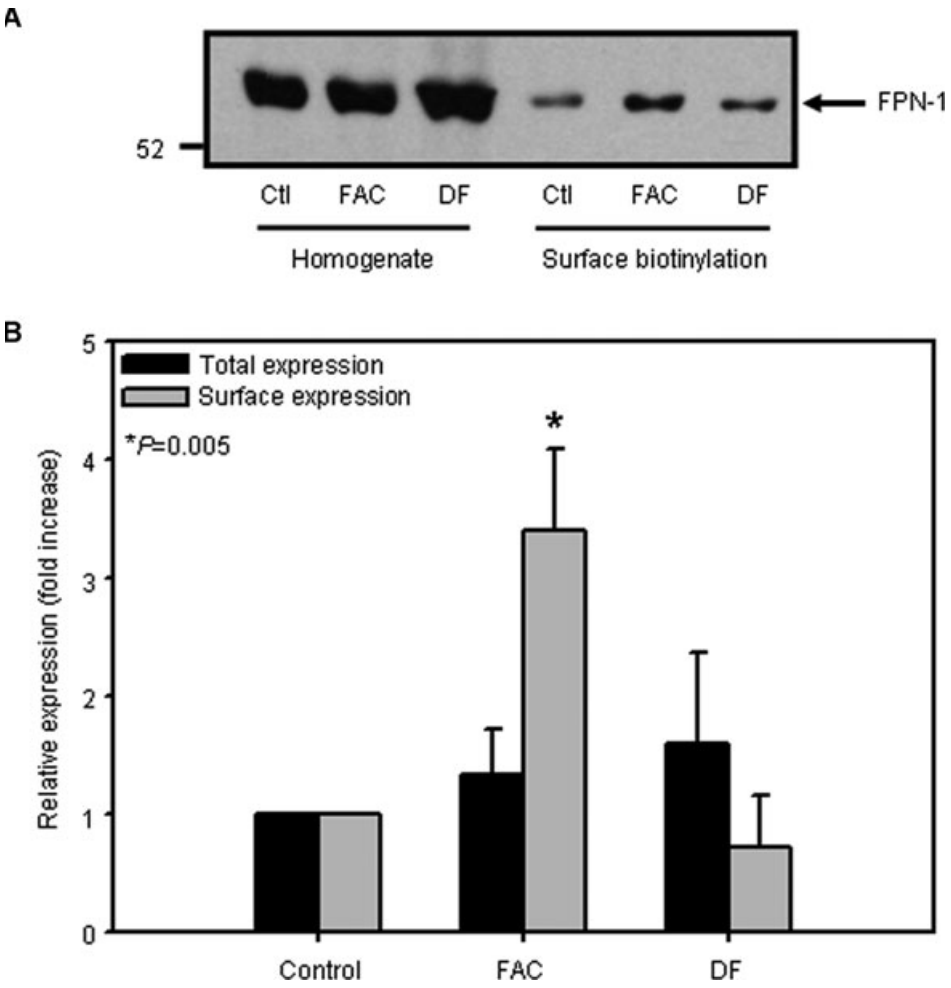

Fig. 4 Immunoblotting of surface biotinylated proteins in WKPT-0293 Cl.2 cells using FPN1 antiserum. (**A**) Lysates or surface biotinylated proteins of non-treated or cells exposed to 100 μM FAC or 100 μM DF for 36 hrs were separated under reducing conditions by SDS-PAGE electrophoresis on an 8% acrylamide gel. The blot was incubated with anti-rat FPN1 (1:500). Characteristic bands at ~60 kD for FPN1 were detected. (**B**) Densitometry analysis was performed and the ratios between FAC- or DF-treated and control samples were calculated for each individual experiment and expressed as fold increase or decrease compared to controls. Means ± S.E.M. of five to nine experiments are shown and significant differences ($P = 0.005$) to controls were calculated using one-way ANOVA (*P*-value for control surface FPN1 expression *versus* DF was 0.710; *P*-values for control total FPN1 expression *versus* FAC and DF were 0.410 and 0.209, respectively).

accession number AF231120) encodes a 570 amino acid protein with a predicted molecular weight of 62 kD. Therefore, taking the limits of molecular weight determination by SDS-PAGE into account, Liu-FPN1 detects a protein of the correct size corresponding to FPN1.

Using Liu-FPN1 for immunoblotting of kidney cortex, outer medulla and inner medulla protein extracts revealed that the 60 kD FPN1 protein was expressed in cortex and outer medulla and only slightly in inner medulla, which indicates that FPN1 is also expressed in the medullary portions of the nephron, as suggested by others in mice [40]. Recently, Zhang *et al.* identified a novel FPN1 transcript (FPN1B) that lacks an iron-responsive element and is specifically expressed in duodenum and is not expressed at detectable amounts in the kidney [41]. The two FPN1 mRNAs, FPN1A (IRE) and FPN1B (non-IRE) encode the same sized protein and therefore this is unlikely to explain the 60 and 65 kD bands observed in immunoblots (Fig. 1B). It is possible that the 65 kD band represents a phosphorylated form of the 60 kD protein, although this needs to be tested in future experiments. Interestingly, a ~110 kD protein band was also detected in all three kidney regions. This larger protein band could represent a dimer of FPN1, although why this signal was not observed in duodenum despite the fact that all protein samples were subjected to the same treatment remains unclear (we incubated samples at 65°C for 10 min. because boiling is known to enhance higher molecular weight forms of FPN1 (see for instance [42] as opposed to [43])). FPN1 has been suggested to function as a monomer [39, 44] or as a homodimer [44, 45]. Our data support both notions, and point to the possibility that the quaternary structure of FPN1 may differ between tissues.

Immunoperoxidase staining of kidney sections using Liu-FPN1 revealed FPN1 expression on the basal and lateral membranes of PT cells in the order S2 > S1 > S3 PT segments. This was confirmed by immunogold electron microscopy. Importantly, no staining of the apical membrane was observed with either technique indicating that FPN1 is unlikely to be involved in translocation of iron across the apical brush-border membrane in animals in iron balance. Expression of an iron transporter protein in the BLM is a prerequisite for vectorial transport of iron from urine to blood and the finding that FPN1 localizes to the BLM of PT cells fulfils this requirement [21].

A recent study in mice has suggested that FPN1 is mainly expressed intracellularly beneath the apical and BLMs of S1- and S2-segment kidney PT [40]. Anaemia was observed to increase FPN1 expression in these nephron segments and cause redistribution of FPN1 to the apical membrane. Functionally, this would suggest that FPN1 exports iron out of PT cells across the apical membrane to reduce intracellular iron concentration and favour iron excretion in anaemic animals.

Our second aim was therefore to test the effect of increasing or reducing cellular iron concentration on PT FPN1. Exposing cells *in vitro* to FAC caused a significant increase in cellular iron concentration, but had no detectable effect on the total amount of FPN1 expressed in PT cells. However, FAC treatment caused a dramatic increase in the surface expression of FPN1 indicating that FPN1 had trafficked to the plasma membrane. We suggest that this may represent a response to protect PT cells against damaging concentrations of intracellular iron. However, we make this suggestion with caution bearing in mind that the major regulator of FPN1, hepcidin was not present in our experiments with cultured cells, therefore it remains to be determined if our observation reflects the renal response to iron excess *in vivo* in an hepcidin replete setting. Interestingly, FAC did not affect FPN1 mRNA or protein expression in cultured PT cells (Fig. 4 and data not shown) though this treatment was effective in raising cellular iron content ~6-fold above control cell iron concentration.

Treatment with DF was found to significantly reduce cellular iron content by ~25% compared to control cells. However, despite this small but consistent reduction in cellular iron we did not detect a change in either FPN1 mRNA or protein levels. These data, together with the data from the FAC experiments, suggest that in WKPT cells FPN1 mRNA and protein levels may not be responsive to altered iron concentration. We cautiously draw this conclusion bearing in mind that the changes in cellular iron concentration we induced may not have been sufficient to bring about modulation of FPN1 mRNA or protein.

Previously we have shown that feeding rats an iron enriched diet or an iron deficient diet alters expression of DMT1 in PT [11]. Dietary loading of iron was found to cause a decrease in PT DMT1 expression, whereas dietary iron restriction caused an increase in DMT1 expression. In PT cells DMT1 is expressed in the membranes of late endosomes and lysosomes [11]. Extracellular addition of transferrin to the apical membrane results in uptake of transferrin, followed by trafficking of transferrin to late endosomes and lysosomes where it colocalizes with DMT1 [11, 12]. We suggest that this mechanism represents the entry route of transferrin bound iron taken up from the urine, possible in the first instance by transferrin receptor 1 and or cubilin expressed in the apical brush border [19, 20]. DMT1 then transports the iron into the PT cell across the late endosomal and lysosomal membranes. From our data detailing the expression of FPN1 in PT cells we can speculate that iron may then transit to the BLM and be exported back into the circulation *via* FPN1.

In conclusion we have developed an affinity purified antisera that specifically recognizes rat FPN1. In rat kidney PT FPN1 is expressed on the BLM of S1, S2 and S3 segments. Under conditions of increased cellular iron, intracellularly expressed FPN1 traffics to the plasma membrane. We suggest that these data indicate that iron is vectorially transported across PT cells in urine to blood direction and this may represent a hitherto undescribed mechanism for salvaging iron filtered by the glomerulus.

Acknowledgements

This work was supported by the Deutsche Forschungsgemeinschaft (grants TH 345 10–1 and 11–1 to F.T.), Kidney Research UK (C.P.S.) and the Wellcome Trust (C.P.S.).

Supporting Information

Additional Supporting Information may be found in the online version of this article:

Fig. S1 Characterization of Liu-FPN1antiserum. (**A**) Immunoblotting of rat duodenal membranes using Liu-FPN1antiserum separated by SDS-PAGE on a 12% acrylamide gel shows an immunoreactive band at 60 kD. The signal was not observed following pre-incubation of the antiserum with immunizing peptide (25 μg/ml). (**B**) and (**C**): Oocytes injected with rat FPN1 cRNA (**B**) or H_2O (**C**) were cryosectioned and incubated with a 1:100 dilution of Liu-FPN1 and then Alexa 594 labelled secondary antibody. Membranes of rat FPN1 cRNA injected oocytes were strongly stained. (**D**) and (**E**): Immunoperoxidase staining of 5 μm paraffin section of rat duodenum showing staining with Liu-FPN1 observed in duodenal villi cells (**D**, ×200 magnification). No signal was detected by pre-incubation of the antiserum with peptide (25 μg/ml) as shown in the inset in the panel. At higher magnification (**E**, ×800 magnification), the staining with Liu-FPN1 antiserum was observed on the BLMs (red arrow head) of the duodenal enterocytes. No staining was detected on the apical membrane (cyan arrow). L = duodenal lumen.

Fig. S2 Immunogold electron microscopy of Liu-FPN1 in rat kidney. (**A**) Overview of a cell from a PT S3 segment. The boxes indicate the area shown at high magnification in (**B**) and (**C**). In S3 PT cells immunogold labelling of FPN1 is observed throughout the basolateral plasma membrane domains (arrows). Gold particles are 10 nm.

Please note: Wiley-Blackwell are not responsible for the content or functionality of any supporting materials supplied by the authors. Any queries (other than missing material) should be directed to the corresponding author for the article.

References

1. **McKie AT, Marciani P, Rolfs A, *et al.*** A novel duodenal iron-regulated transporter, IREG1, implicated in the basolateral transfer of iron to the circulation. *Mol Cell*. 2000; 5: 299–309.
2. **Donovan A, Brownlie A, Zhou Y, *et al.*** Positional cloning of zebrafish ferroportin1 identifies a conserved vertebrate iron exporter. *Nature*. 2000; 403: 776–81.
3. **Abboud S, Haile DJ.** A novel mammalian iron-regulated protein involved in intracellular iron metabolism. *J Biol Chem*. 2000; 275: 19906–12.
4. **Canonne-Hergaux F, Donovan A, Delaby C, *et al.*** Comparative studies of duodenal and macrophage ferroportin proteins. *Am J Physiol Gastrointest Liver Physiol*. 2006; 290: G156–63.
5. **De Domenico I, Ward DM, Langelier C, *et al.*** The molecular mechanism of hepcidin-mediated ferroportin down-regulation. *Mol Biol Cell*. 2007; 18: 2569–78.
6. **De Domenico I, Ward DM, Nemeth E, *et al.*** The molecular basis of ferroportin-linked hemochromatosis. *Proc Natl Acad Sci USA*. 2005; 102: 8955–60.
7. **Nemeth E, Tuttle MS, Powelson J, *et al.*** Hepcidin regulates cellular iron efflux by binding to ferroportin and inducing its internalization. *Science*. 2004; 306: 2090–3.
8. **Thomas C, Oates PS.** IEC-6 cells are an appropriate model of intestinal iron absorption in rats. *J Nutr*. 2002; 132: 680–7.
9. **Donovan A, Lima CA, Pinkus JL, *et al.*** The iron exporter ferroportin/Slc40a1 is essential for iron homeostasis. *Cell Metab*. 2005; 1: 191–200.
10. **Vulpe CD, Kuo YM, Murphy TL, *et al.*** Hephaestin, a ceruloplasmin homologue implicated in intestinal iron transport, is defective in the sla mouse. *Nat Genet*. 1999; 21: 195–9.
11. **Wareing M, Ferguson CJ, Delannoy M, *et al.*** Altered dietary iron intake is a strong modulator of renal DMT1 expression. *Am J Physiol Renal Physiol*. 2003; 285: F1050–9.
12. **Abouhamed M, Gburek J, Liu W, *et al.*** Divalent metal transporter 1 in the kidney proximal tubule is expressed in late endosomes/lysosomal membranes: implications for renal handling of protein-metal complexes. *Am J Physiol Renal Physiol*. 2006; 290: F1525–33.
13. **Abouhamed M, Wolff NA, Lee WK, *et al.*** Knockdown of endosomal/lysosomal divalent metal transporter 1 by RNA interference prevents cadmium-metallothionein-1 cytotoxicity in renal proximal tubule cells. *Am J Physiol Renal Physiol*. 2007; 293: F705–12.
14. **Wareing M, Ferguson CJ, Green R, *et al.*** *In vivo* characterization of renal iron transport in the anaesthetized rat. *J Physiol*. 2000; 524: 581–6.
15. **Bohrer MP, Deen WM, Robertson CR, *et al.*** Influence of molecular configuration on the passage of macromolecules across the glomerular capillary wall. *J Gen Physiol*. 1979; 74: 583–93.
16. **Ohlson M, Sorensson J, Haraldsson B.** A gel-membrane model of glomerular charge and size selectivity in series. *Am J Physiol Renal Physiol*. 2001; 280: F396–405.
17. **Deen WM, Bridges CR, Brenner BM, *et al.*** Heteroporous model of glomerular size selectivity: application to normal and nephrotic humans. *Am J Physiol*. 1985; 249: F374–89.
18. **Koshimura J, Narita T, Sasaki H, *et al.*** Urinary excretion of transferrin and orosomucoid are increased after acute protein loading in healthy subjects. *Nephron Clin Pract*. 2005; 100: c33–7.
19. **Zhang D, Meyron-Holtz E, Rouault TA.** Renal iron metabolism: transferrin iron delivery and the role of iron regulatory proteins. *J Am Soc Nephrol*. 2007; 18: 401–6.
20. **Kozyraki R, Fyfe J, Verroust PJ, *et al.*** Megalin-dependent cubilin-mediated endocytosis is a major pathway for the apical uptake of transferrin in polarized epithelia. *Proc Natl Acad Sci USA*. 2001; 98: 12491–6.
21. **Smith CP, Thévenod F.** Iron transport and the kidney. *Biochim Biophys Acta*. 2009; 1790: 724–30.
22. **Roussa E, Nastainczyk W, Thevenod F.** Differential expression of electrogenic NBC1 (SLC4A4) variants in rat kidney and pancreas. *Biochem Biophys Res Commun*. 2004; 314: 382–9.
23. **Stewart GS, Graham C, Cattell S, *et al.*** UT-B is expressed in bovine rumen: potential role in ruminal urea transport. *Am J Physiol Regul Integr Comp Physiol*. 2005; 289: R605–12.
24. **Kinne-Saffran E, Kinne RK.** Isolation of lumenal and contralumenal plasma membrane vesicles from kidney. *Methods Enzymol*. 1990; 191: 450–69.
25. **Scalera V, Huang YK, Hildmann B, *et al.*** A simple isolation method for basal-lateral plasma membranes from rat kidney cortex. *Membr Biochem*. 1981; 4: 49–61.
26. **Bradford MM.** A rapid and sensitive method for the quantitation of microgram quantities of protein utilizing the principle of protein-dye binding. *Anal Biochem*. 1976; 72: 248–54.
27. **Fenton RA, Brond L, Nielsen S, *et al.*** Cellular and subcellular distribution of the type-2 vasopressin receptor in the kidney. *Am J Physiol Renal Physiol*. 2007; 293: F748–60.
28. **Moeller HB, Knepper MA, Fenton RA.** Serine 269 phosphorylated aquaporin-2 is targeted to the apical membrane of collecting duct principal cells. *Kidney Int*. 2009; 75: 295–303.
29. **Wolff NA, Abouhamed M, Verroust PJ, *et al.*** Megalin-dependent internalization of cadmium-metallothionein and cytotoxicity in cultured renal proximal tubule cells. *J Pharmacol Exp Ther*. 2006; 318: 782–91.
30. **Woost PG, Orosz DE, Jin W, *et al.*** Immortalization and characterization of proximal tubule cells derived from kidneys of spontaneously hypertensive and normotensive rats. *Kidney Int*. 1996; 50: 125–34.
31. **Hirsh M, Konijn AM, Iancu TC.** Acquisition, storage and release of iron by cultured human hepatoma cells. *J Hepatol*. 2002; 36: 30–8.
32. **Hubert N, Hentze MW.** Previously uncharacterized isoforms of divalent metal transporter (DMT)-1: implications for regulation and cellular function. *Proc Natl Acad Sci USA*. 2002; 99: 12345–50.
33. **Qian M, Liu M, Eaton JW.** Transition metals bind to glycated proteins forming redox active "glycochelates": implications for the pathogenesis of certain diabetic complications. *Biochem Biophys Res Commun*. 1998; 250: 385–9.
34. **Gao X, Campian JL, Qian M, *et al.*** Mitochondrial DNA damage in iron overload. *J Biol Chem*. 2009; 284: 4767–75.
35. **Lowry O, Rosebrough N, Farr A, *et al.*** Protein measurements with the Folin phenol reagent. *J Biol Chem*. 1951; 194: 265–75.
36. **Schmitt BM, Biemesderfer D, Romero MF, *et al.*** Immunolocalization of the electrogenic Na^{+}-HCO^{-3} cotransporter in mammalian and amphibian kidney. *Am J Physiol*. 1999; 276: F27–38.

37. **Canonne-Hergaux F, Gros P.** Expression of the iron transporter DMT1 in kidney from normal and anemic mk mice. *Kidney Int*. 2002; 62: 147–56.
38. **Wu LJ, Leenders AG, Cooperman S, *et al.*** Expression of the iron transporter ferroportin in synaptic vesicles and the blood-brain barrier. *Brain Res*. 2004; 1001: 108–17.
39. **Goncalves AS, Muzeau F, Blaybel R, *et al.*** Wild-type and mutant ferroportins do not form oligomers in transfected cells. *Biochem J*. 2006; 396: 265–75.
40. **Veuthey T, D'Anna MC, Roque ME.** Role of the kidney in iron homeostasis: renal expression of Prohepcidin, Ferroportin, and DMT1 in anemic mice. *Am J Physiol Renal Physiol*. 2008; 295: F1213–21.
41. **Zhang DL, Hughes RM, Ollivierre-Wilson H, *et al.*** A ferroportin transcript that lacks an iron-responsive element enables duodenal and erythroid precursor cells to evade translational repression. *Cell Metab*. 2009; 9: 461–73.
42. **Yang F, Liu XB, Quinones M, *et al.*** Regulation of reticuloendothelial iron transporter MTP1 (Slc11a3) by inflammation. *J Biol Chem*. 2002; 277: 39786–91.
43. **Knutson MD, Oukka M, Koss LM, *et al.*** Iron release from macrophages after erythrophagocytosis is up-regulated by ferroportin 1 overexpression and down-regulated by hepcidin. *Proc Natl Acad Sci USA*. 2005; 102: 1324–8.
44. **Pignatti E, Mascheroni L, Sabelli M, *et al.*** Ferroportin is a monomer *in vivo* in mice. *Blood Cells Mol Dis*. 2006; 36: 26–32.
45. **De Domenico I, Ward DM, Musci G, *et al.*** Evidence for the multimeric structure of ferroportin. *Blood*. 2007; 109: 2205–9.